ON THE SOLUTION OF ASYMPTOTIC IMPACT PROBLEMS WITH SIGNIFICANT LOCALISED INDENTATION

[1]Akuro Big-Alabo[a], Matthew P. Cartmell[b], and Philip Harrison[a]

[a] Systems, Power and Energy Research Division, School of Engineering, University of Glasgow, G12 8QQ, Scotland, UK

[b] Department of Mechanical Engineering, University of Sheffield, Mappin Street, Sheffield, S1 3JD, England, UK

Abstract

A major challenge in studying impact problems analytically is solving the governing equations of impact events, which are mostly in the form of nonlinear ODEs. This paper focuses on the solution of nonlinear models for impact problems in asymptotic cases, where local indentation is significant. The asymptotic cases consist of both half-space and infinite plate impacts, which cover a wide range of practical impact events. A so-called *force-indentation linearisation method* (FILM), first described in a previous study, is reformulated here in a more general form in order to broaden its scope of application. The generalisation of the FILM facilitates stable and convergent solutions even when complex nonlinear contact models are used to estimate the impact force. Simulations based on the FILM approach are validated using numerical solutions.

Keywords: *contact model, asymptotic impact, indentation, elastoplastic impact, force-indentation linearisation method, numerical integration*.

[1] Corresponding author - E: akuro.big-alabo@uniport.edu.ng; T: +44 777 427 9617

1. Introduction

Many engineering structures made of metals or composite materials are used in environments where they are exposed to impact of freely flying projectiles. For example, impact of runway debris on an airplane body, object dropping on a car body or platform, impact of space structures by space debris, hailstone impact, etc. The low-velocity impact of a structure by a rigid projectile normally results in plastic deformation and/or damage of the structure [1 - 3], and this reduces the performance of the structure. For metallic targets, low-velocity impact results in plastic deformation, which gives rise to a permanent indentation at the end of the impact unloading. On the other hand, low-velocity impact of targets made of composite material results in plastic deformation of the matrix and damage of the fibre in the form of debonding, breakage, kinking, micro-buckling, etc. This means that models for analysis of low-velocity impact events should account for elastoplastic (post-yield deformation) effects i.e. plastic deformation and/or damage.

The impact force and the local indentation during low- to medium-velocity impact are determined using quasi-static assumptions [1], and therefore estimated using an appropriate static contact model. Static contact models that account for elastoplastic effects have been developed for metallic targets [1, 2, 4 - 6] and for composite laminate targets [3, 7, 8]. Contact models can be divided into two general groups according to the compliance relationships used to model the various indentation stages, namely: Meyer type and non-Meyer type. Meyer type contact models are defined here as those in which the compliance relationships for all the indentation stages are expressed as [2]:

$$F = K_c \delta^q \tag{1}$$

where K_c is the contact stiffness and $q \geq 1$ is a number defining the power law relationship between the contact force and indentation. Specific models can be derived from this general Meyer-type form by using a given parameter set. For example, the Hertz contact model is a specific form of Meyer contact model with K_c equal to the Hertzian contact stiffness and $q = 3/2$. On the other hand, non-Meyer type contact models use compliance relationships that cannot be expressed in terms of equation (1) in at least one indentation stage (usually the elastoplastic indentation stage). For example, the compliance model for the elastoplastic indentation stage of the contact model of Stronge [4], see equation (2), cannot be expressed in terms of equation (1). Hence, Stronge's contact model is a non-Meyer type contact model.

$$F = F_y \left(\frac{2\delta}{\delta_y} - 1\right)\left[1 + \frac{1}{3.3} ln\left(\frac{2\delta}{\delta_y} - 1\right)\right] \qquad \delta_y \leq \delta \leq \delta_p \tag{2}$$

Other examples of non-Meyer type contact models include the elastoplastic contact models in references [1, 5, 9, 10]. Impact models incorporating non-Meyer type contact models usually take relatively complex forms and are therefore more challenging to solve [11].

Although the indentation response of metals during the elastoplastic loading stage is nonlinear [1, 2, 4, 8], some linear elastoplastic compliance models have been used to provide good predictions when compared with limited experimental measurements [2] and finite element results [12]. Linear elastoplastic compliance models are normally used to overcome computational difficulties associated with integrating impact models incorporating nonlinear elastoplastic contact models. Nevertheless, nonlinear elastoplastic contact models tend to be more reliable and more physically consistent than analogous linear approximations and are therefore required for proper theoretical analysis of half-space impacts.

Nonlinear elastoplastic contact models are usually of the non-Meyer type and despite the success and wide use of the latter for static indentation analyses [1, 4, 10], studies in which such models have been used to investigate the response history of elastoplastic half-space impacts are scarce. A possible explanation is the computational challenge involved; an attempt by the current authors [11] to use Stronge's non-Meyer type contact model [4] to investigate an elastoplastic impact event revealed convergence problems when using a cubic Hermit interpolation method in NDSolve function of Mathematica™. Such problems were avoided when using a Meyer-type contact model [6]. It can be concluded that there is a need either to develop Meyer type contact models for the elastoplastic loading stage, or alternatively, to develop more efficient and robust solution algorithms able to solve the highly nonlinear ODEs associated with non-Meyer type contact models. Addressing this latter goal is one of the main aims of this investigation.

Analytical models for low-velocity impact of a target by a rigid spherical projectile are normally formulated using the equations of motion of the contacting bodies and a static contact model that accounts for the local indentation. In general, impact models for spherical impact of transversely flexible targets account for the vibrations of the target, local indentation and boundary conditions, and are reducible to a set of coupled nonlinear ODEs. In contrast, the impact models for spherical impact of transversely inflexible targets are in the form of single degree-of-freedom nonlinear ODEs. The geometrical features of the target relative to the spherical projectile may allow use of simplifying assumptions that leads to asymptotic impact models. Three geometric conditions are identified in the literature that can be modelled using asymptotic impact models [13, 14]. The first condition applies when the target is very thick compared to the size of the projectile. This means that the target is transversely inflexible and its

transverse oscillations can be neglected. This kind of impact event can be modelled as a half-space impact. The second condition is when the mass and size of the projectile is very small compared to the mass and planar dimensions of a transversely flexible target. In this case, the impact duration is shorter than the time it will take for the first reflected vibration wave to reach the impact zone. The implication is that the boundary conditions do not affect the impact response. The impact event can be modelled as an infinite plate impact and has been referred to as small mass impact [15] or wave-controlled impact [16]. The third condition is when mass of the projectile is larger than the mass of a transversely flexible target. The vibrations of the target occur quasi-statically and the impact response is influenced by the boundary conditions. The local indentation is negligible compared to the vibration amplitude of the target. The impact event can be modelled using the assumptions of quasi-static bending and the energy-balance principle [16], and has been referred to as large mass impact [15].

All three asymptotic impact events are modelled using single degree-of-freedom ODEs [16]. Of the three asymptotic impact events described above, the half-space and infinite plate response are characterised by significant local indentation, while the impact event with quasi-static bending response is characterised by negligible local indentation. Therefore, the half-space and infinite plate impacts can be referred to as ‘asymptotic impact events with significant local indentation’ and are the focus of this particular investigation. The models for asymptotic impact events with significant local indentation incorporate static indentation models, which are usually nonlinear compliance models, to estimate the impact force and account for the local indentation effects. Hence, the final models for half-space and infinite plate impacts are usually in the form of nonlinear ODEs, except for cases where linearised contact models are used to

estimate the impact force. The latter can be used for qualitative analysis [13, 14], but where quantitative estimates are required the use of linearised contact models, which are approximations to the actual contact behaviour, could lead to significant errors in the predicted response [13]. Since asymptotic impact events with significant local indentation occur in many practical situations, the solution to the models describing the response of these impact events is very important.

Solution of the nonlinear models for asymptotic impact events with significant local indentation may be achieved by conventional numerical schemes such as the small-increment integration method [2] and the Newmark integration method [16], and by robust numerical integration solvers in computational software packages such as the NDSolve function in *Mathematica*™ [11, 17, 18]. Note that the NDSolve function solves a nonlinear ODE by means of an optimised algorithm that selects the best numerical method to use from a set of embedded conventional numerical schemes [17]. Hence, issues of stability and convergence associated with the various conventional numerical schemes occasionally arise in the output of the NDSolve function resulting in non-convergent solutions. Thus, the conditional stability of conventional numerical schemes make them challenging to use, and when convergence can be achieved, often require a large number of iterations to obtain accurate results.

Recently, an analytical algorithm for the solution of nonlinear ODEs governing an elastoplastic half-space impact was developed [18]. The algorithm, which is called the *Force-Indentation Linearisation Method* (FILM), used closed-form solutions derived from piecewise linearisation of the nonlinear force-indentation relationship (compliance model) to determine the response of a half-space impact. The limitations associated with conventional numerical methods discussed above were found to be completely eliminated when using the FILM. In this prior work,

formulation and application of the FILM were limited to half-space impact events modelled using specific Meyer type contact models. It was suggested that future work could focus on extending the FILM to solve the response of half-space impact events modelled using non-Meyer type contact models. In this investigation, this prior suggestion has been implemented and additionally, the FILM has been further extended to solve the nonlinear ODEs governing infinite plate impacts. The goal is to demonstrate how the FILM can be used as an efficient and reliable algorithm, able to solve nonlinear ODEs governing asymptotic impact events involving significant local indentation.

The remainder of the paper is structured as follows. In section 2, the concept of the FILM is formulated mathematically based on a general nonlinear contact model, which can be either Meyer type or non-Meyer type. Also, the distinction between the FILM and nonlinear FEA on one hand, and the FILM and conventional time-integration numerical schemes on the other hand is discussed. Section 3 discusses the application of the FILM to solve the governing nonlinear ODEs of an elastoplastic half-space impact with impact stages incorporating either Meyer type or non-Meyer type models. A FILM solution for the governing ODE of a half-space impact stage modelled based on a modified Meyer-type contact law is presented. Furthermore, an illustration of how the generalised formulation of the FILM discussed in Section 2 can be used to solve the governing ODE of a half-space impact stage incorporating a non-Meyer type contact model is presented. Section 4 discusses the application of the FILM approach to solve nonlinear ODEs governing infinite plate impacts and Section 5 discusses the conclusions of the paper.

2. Generalisation of the FILM

The concept of the FILM is explained in reference [18] and briefly summarised here. Basically, the idea of the FILM is to discretise the nonlinear compliance model used to estimate the impact force into a finite number of segments, and to linearise each of these segments. The linearised segments are used to develop linearised response models that approximate the impact response for each discretisation. Hence, the closed-form solutions of the linearised response models provide approximate solutions of the impact response. In this section, the FILM is formulated based on a general nonlinear compliance model that can represent both Meyer type and non-Meyer type compliance models (see Figure 1). This general formulation allows for a broader application of the FILM.

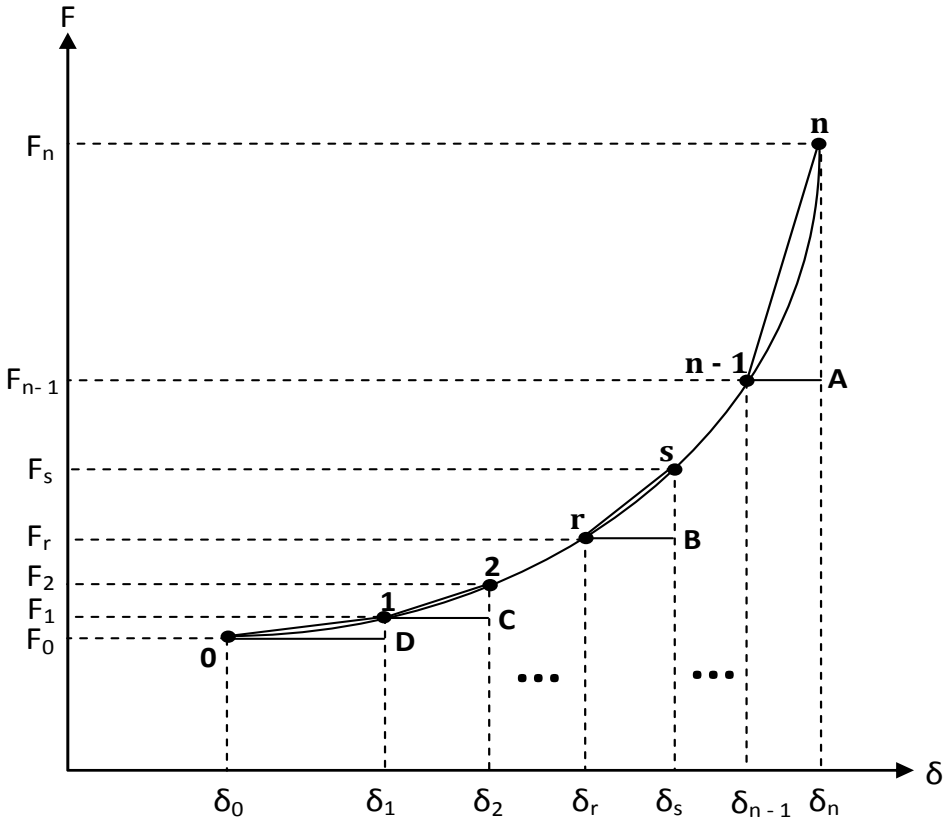

Figure 1: *Piecewise discretisation of a general nonlinear compliance model.*

2.1. Difference between FILM and conventional numerical schemes

The FILM is based on continuous piecewise linearisation of the constitutive nonlinear force-displacement relationship describing the indentation process. A similar piecewise linearisation approach (i.e. tangent or secant stiffness approach) is normally used in FEA to solve the nonlinear equations governing static and dynamic processes [19, 20]. As a result, it is necessary to clarify the difference between the FILM and the tangent or secant stiffness approach used in nonlinear FEA. In nonlinear dynamic FEA, a load increment is assumed for each time increment and the corresponding actual increase in displacement is obtained through an iterative process, such as Newton-Raphson, modified Newton-Raphson or Riks-Wempner method [20], using a tangent or secant stiffness or a combination of both [19]. On the other hand, the FILM involves discretisation of the nonlinear force-indentation relationship using predetermined indentation increments. For each discretisation, a linearised force-indentation relationship is derived to approximate the nonlinear force-indentation relationship, thus leading to the formulation of linearised impact models for each discretisation. Accordingly, closed-form solutions of the linearised impact models are obtained to determine the time-dependent response for each discretisation. Therefore, in contrast to nonlinear dynamic FEA where an iterative process is used to determine the load-displacement equilibrium, the FILM requires no such iterative process and the load-displacement equilibrium is inherent in its formulation. This is the case because the actual load increments corresponding to the predetermined indentation increments are used to formulate the linearised models for each discretisation.

Table 1: Qualitative difference between the FILM and conventional numerical schemes for solving nonlinear half-space impact models

	FILM	Conventional numerical schemes
1	The force is discretised in terms of a dependent variable i.e. indentation.	The force or variable of interest is discretised in terms of the independent variable i.e. time.
2	Produces closed-form solutions used to approximate the actual solution.	Produces numerical solutions used to approximate the actual solution.
3	Closed-form solutions are derived analytically and do not require any iterations.	Numerical solutions require iterations and an error condition to terminate the iterations.
4	Each closed-form solution applies to a range of time of the impact duration.	Each numerical solution applies to a discrete time of the impact duration.
5	Requires very few discretisations of the impact force to obtain sufficiently accurate solutions; typically 5 to 10 discretisations.	Requires many discretisations of the impact force or variable of interest; usually multiples of 10 to hundreds.
6	Produces solution with the same relative computational effort notwithstanding the complexity of the nonlinearity in the impact model.	The computational effort increases with the complexity of the nonlinearity in the impact model.
7	Easy to implement by hand calculation.	Computer implementation is required.
8	Inherently stable for solution of the nonlinear ODEs governing half-space impact.	Conditionally stable for the solution of the nonlinear ODEs governing half-space impact.
9	Convergence of solution for half-space impact models incorporating non-Meyer type contact models is always guaranteed.	Convergence of solution for half-space impact models incorporating non-Meyer type contact models is not always guaranteed [11].

Having made the distinction between the FILM and the nonlinear FEA procedures, it is also important to distinguish between the FILM and the numerical

time-integration schemes that are normally used to solve nonlinear half-space impact models. The main differences between the FILM and the conventional numerical time-integration schemes are summarised in Table 1 and is intended to highlight why the FILM is preferable for the solution of half-space impact problems compared to the conventional numerical time-integration schemes. Although the FILM was originally formulated for the solution of half-space impact models, its application to solve nonlinear models of infinite plate impact is also examined later in this paper.

2.2. Mathematical formulation of the FILM for a general nonlinear compliance model

Assuming that $F(\delta)$ is a nonlinear function of δ as shown in Figure 1 and $F_i = F(\delta_i)$ where i represents any point on the nonlinear force-indentation curve. Then from Figure 1, F_{01} = slope of $\overline{01} \times (\delta_{01} - \delta_0) + F_0$ where F_{01} is the linearised force for the segment of $F(\delta)$ between point 0 and point 1. Hence,

$$F_{01} = \frac{F_1 - F_0}{\delta_1 - \delta_0}(\delta_{01} - \delta_0) + F_0 = \frac{F(\delta_1) - F(\delta_0)}{\delta_1 - \delta_0}(\delta_{01} - \delta_0) + F(\delta_0) \qquad (3a)$$

Similarly,

$$F_{12} = \frac{F(\delta_2) - F(\delta_1)}{\delta_2 - \delta_1}(\delta_{12} - \delta_1) + F(\delta_1) \qquad (3b)$$

And generally,

$$F_{rs} = \frac{F(\delta_s) - F(\delta_r)}{\delta_s - \delta_r}(\delta_{rs} - \delta_r) + F(\delta_r) \qquad (4)$$

where $r = 0, 1, 2, 3, \dots, n-1$ and $s = r + 1$ are the initial and end states of each segment respectively. During unloading $r = n, n-1, n-2, \dots, 3, 2, 1$ are the initial states while $s = r - 1$ are the end states. F_{rs} is the linearised force for each segment and it can be rewritten as:

$$F_{rs} = K_{rs}(\delta_{rs} - \delta_r) + F(\delta_r) \tag{5}$$

where

$$K_{rs} = \frac{F(\delta_s) - F(\delta_r)}{\delta_s - \delta_r} \tag{6}$$

Supposing each segment has an equal indentation range i.e. $\Delta\delta = \delta_s - \delta_r$ is constant, then δ_r can be expressed for n segments as:

$$\delta_r = \delta_0 + r(\delta_n - \delta_0)/n \tag{7}$$

When the linearised contact force (equation (5)) is substituted in the dynamic equation of a half-space impact, a linear differential equation is obtained from which closed-form solutions can be derived for each segment. This general formulation, combined with the energy balance principle [6], can be used to derive the complete solution of a rate-independent half-space impact irrespective of the nature of nonlinearity in the compliance model used to estimate the impact response.

3. Impact of a half-space target by a rigid spherical projectile

A half-space target is one that has an infinite thickness. It is an analytical idealisation that can be used to represent very thick targets impacted by projectiles with relatively small size and mass. Such targets are considered to be transversely inflexible and their vibrations are negligible, if any. Therefore, the local indentation is determined by the displacement of the projectile. The impact energy is essentially used for local indentation of the target as other possible forms of dissipations such as elastic waves, sound and friction can be safely neglected for low- to medium-velocity impacts [1]. Half-space impact conditions are normally used in experiments and finite element analysis to determine the response during dynamic indentation e.g. coefficient of restitution and contact

time [9, 21, 22] and the material properties of the target e.g. dynamic yield [4, 23]. The impact response of a half-space target struck by a rigid spherical impactor is modelled by a single degree-of-freedom motion as shown in equation (8).

$$m\ddot{\delta} + F = 0 \tag{8}$$

where m is the mass of the projectile; δ is the indentation, which is equal to the displacement of the projectile; the initial conditions are $\delta(0) = 0$ and $\dot{\delta}(0) = V_0$; $F = F(\delta) \geq 0$ is the impact force, which is estimated from a static contact model.

3.1. Half-space impact modelled using a generalised Meyer type contact law and solved using the FILM

Big-Alabo *et al* [18] applied the FILM to derive solutions for two examples of half-space impact modelled using specific Meyer type contact models i.e. the Hertz contact model for elastic impact and the contact model of Majeed *et al* [8] for elastoplastic impact. In this section, a FILM solution is derived for the response of a half-space impact stage that is modelled based on a general Meyer type contact law (see equation (1)), rather than specific instances of the latter. This FILM solution has the important advantage that it eliminates the need to develop a FILM solution from first principle, for each specific Meyer type contact model considered.

Meyer's law is considered the general form for most static contact models [2]. A modified form of Meyer's law incorporating post-yield effects can be written as:

$$F = K_c(\delta - \delta_0)^q + F_0 \tag{9}$$

where δ_0 and F_0 are the indentation and contact force at the onset of a loading or unloading stage. During elastic impact response $\delta_0 = 0$ and $F_0 = 0$, while for post-elastic impact response, $\delta_0 \neq 0$ and $F_0 \neq 0$. Therefore, the model for a half-space

impact governed by a Meyer type contact law accounting for post-yield effects can be written as:

$$m\ddot{\delta} + K_c(\delta - \delta_0)^q + F_0 = 0 \tag{10}$$

The FILM need only be applied when $q \neq 1$ i.e. when equation (10) is nonlinear. If $q = 1$, then equation (10) is linear and closed-form solutions can be obtained directly without need for the FILM or any other numerical integration scheme.

Substituting equation (9) in equation (5),

$$F_{rs} = \frac{K_c(\delta_s - \delta_0)^q - K_c(\delta_r - \delta_0)^q}{\delta_s - \delta_r}(\delta_{rs} - \delta_r) + K_c(\delta_r - \delta_0)^q + F(\delta_0) \tag{11}$$

From equation (7),

$$\delta_s - \delta_r = \delta_{r+1} - \delta_r = (\delta_n - \delta_0)/n \tag{12}$$

Note that δ_n is the indentation at the end of the loading or unloading stage considered (see Figure 1), and δ_n is obtained from the energy balance algorithm [6] when it is equal to the maximum indentation, otherwise it is obtained from the contact model used to estimate the impact response. Substituting equations (7) and (12) in equation (11), and after algebraic simplifications, the linearised contact force for each discretisation can be written as:

$$F_{rs} = K_{rs}(\delta_{rs} - \delta_r) + K_c(\delta_r - \delta_0)^q + F_0 \tag{13}$$

where

$$K_{rs} = nK_c(\delta_n - \delta_0)^{q-1}\left[\left(\frac{s}{n}\right)^q - \left(\frac{r}{n}\right)^q\right] \tag{14}$$

Substituting equation (13) in equation (8), the governing equation for the impact response of each discretisation is given by:

$$m\ddot{\delta}_{rs} + K_{rs}\delta_{rs} = K_{rs}\delta_r - K_c(\delta_r - \delta_0)^q - F_0 \tag{15}$$

Equation (15) is a non-homogeneous linear differential equation and the complete solution can be readily obtained as:

$$\delta_{rs} = R_{rs}\,\mathrm{Sin}(\omega_{rs}t + \varphi_{rs}) + C_{rs} \tag{16}$$

Taking the first derivative of equation (16), the velocity profile is given by:

$$\dot{\delta}_{rs} = \omega_{rs} R_{rs} \operatorname{Cos}(\omega_{rs} t + \varphi_{rs}) \tag{17}$$

where $R_{rs} = (A_{rs}^2 + B_{rs}^2)^{1/2}$; $C_{rs} = (K_{rs}\delta_r - K_c(\delta_r - \delta_0)^q - F_0)/K_{rs}$; $\omega_{rs} = \sqrt{K_{rs}/m}$; and $\varphi_{rs} = \tan^{-1}(B_{rs}/A_{rs}) - \omega_{rs} t_r$. Using equations (16) and (17), $A_{rs} = \dot{\delta}_r/\omega_{rs}$ and $B_{rs} = \delta_r - C_{rs}$. The constants A_{rs} and B_{rs} depend on the initial conditions, $\delta(t_r) = \delta_r$ and $\dot{\delta}(t_r) = \dot{\delta}_r$, where t_r is calculated as [17]:

$$t_r = \left(\frac{\pi}{2} \pm \operatorname{ArcCos}[(\delta_r - C_{rs})/R_{rs}] - \varphi_{rs}\right)/\omega_{rs} \tag{18}$$

Since the displacements at the boundaries of each discretisation are known i.e. $\delta_r = \delta_0 + r(\delta_n - \delta_0)/n$, then one initial condition is already available. The second initial condition is determined by substituting equation (18) in equation (17). In equation (18), the trigonometric term in the numerator is negative during the loading stage and positive during the restitution stage. The sign change in this term during the restitution stage accounts for the fact that the contact force is reversed. At maximum conditions, this term vanishes so that $t_m = (\pi/2 - \varphi_{rs})/\omega_{rs}$. Equation (18) is used to determine the time boundaries for each discretisation, and then, equations (16), (17) and (13) are used to extract data points for the indentation, velocity and force histories within the time boundaries.

Equations (13, 14, and 16 – 18) constitute the FILM solution for a half-space impact modelled using a general Meyer type contact law. To adapt this solution to the case of a specific Meyer type contact model, the constants δ_0, F_0, δ_n, K_c and q are defined from the contact model and used to re-evaluate equations (7) and (14), and the expression for C_{rs}. For example, during elastic impact of a spherical impactor on a half-space target $\delta_0 = 0$, $F_0 = 0$, $\delta_n = \delta_m$, $K_c = K_h$ and $q = 3/2$. Substituting these values into equations (13, 14, and 16 - 18) the FILM solution for elastic half-space impact derived in reference [18] is obtained.

To further demonstrate the application of the FILM solution derived for the response of a half-space impact modelled using a general Meyer type contact law, the contact model of Big-Alabo *et al* [6] is used to estimate the impact force during the elastoplastic impact of a mild steel slab struck by a spherical tungsten carbide ball. Although this example is qualitatively similar to the elastoplastic impact example investigated in reference [18], it is included here in order to clearly demonstrate the application of the FILM solution in equations (13, 14, and 16 - 18). Furthermore, the elastoplastic loading stage of the example investigated in reference [18] was modelled using a linear Meyer type compliance model, whereas the elastoplastic loading stage of the present example is modelled using a nonlinear Meyer type compliance model.

The contact model of Big-Alabo *et al* [6] has four loading stages; an elastic loading stage, two subsequent elastoplastic loading stages, followed by a fully plastic loading stage. Also, there is a single unloading stage that models the restitution from any of the loading stages. All of these stages are modelled using Meyer type compliance models. Details of the formulation of this contact model can be found in reference [6] and are not repeated here for brevity. The contact model is summarised as follows.

$$F = \begin{cases} K_h \delta^{3/2} & 0 \le \delta \le \delta_y \\ K_h\left(\delta - \delta_y\right)^{3/2} + K_h \delta_y^{3/2} & \delta_y \le \delta \le \delta_{tep} \\ K_l\left(\delta - \delta_{tep}\right) + K_h\left[\left(\delta_{tep} - \delta_y\right)^{3/2} + \delta_y^{3/2}\right] & \delta_{tep} \le \delta \le \delta_p \\ K_p\left(\delta - \delta_p\right) + F_{\delta=\delta_p} & \delta_p \le \delta \le \delta_m \\ K_u\left(\delta - \delta_f\right)^{3/2} & \delta_f \le \delta \le \delta_m \end{cases} \qquad (19a-e)$$

Equations (19a-e) represent the compliance model for the elastic loading, nonlinear elastoplastic loading, linear elastoplastic loading, fully plastic loading and unloading stages respectively. The contact parameters in equations (19a-e) are given as: $K_h = (4/3)ER^{1/2}$ where E and R are the effective modulus and radius

respectively, and are calculated as: $E = [(1-\upsilon_i^2)/E_i + (1-\upsilon_t^2)/E_t]^{-1}$ and $R = [1/R_i + 1/R_t]^{-1}$; the subscripts i and t stand for indenter and target respectively, and υ is the Poisson's ratio; $\delta_y = \left(1.1\pi R S_y/K_h\right)^2$ where S_y is the yield stress of the target; $K_l = 5.40K_h\delta_y^{1/2}$; $\delta_{tep} = 13.93\delta_y$; $K_p = 4.6\pi R S_y$; $\delta_p = 82.5\delta_y$; $F_{\delta=\delta_p} = 70.0K_l\delta_y + 47.6K_h\delta_y^{3/2}$; $K_u = (4/3)ER_d^{1/2}$; $\delta_f = \delta_m - \left(3F_m/4ER_d^{1/2}\right)^{2/3}$ where R_d is the deformed effective radius, and $R_d \geq R$; δ_m and F_m are the maximum indentation and impact force, which are determined using the energy balance algorithm in [6]. The deformed effective radius is calculated as [24, 25]:

$$\left.\begin{array}{ll} R_d = R & 0 \leq \delta_m \leq \delta_y \\ R_d = \left[\left(\dfrac{\delta_m - \delta_y}{\delta_{tep} - \delta_y}\right)^{3/2} + 1\right]R & \delta_y \leq \delta_m \leq \delta_{tep} \\ R_d = \left[0.8\left(\dfrac{\delta_m - \delta_{tep}}{\delta_p - \delta_{tep}}\right) + 2\right]R & \delta_{tep} \leq \delta_m \leq \delta_p \\ R_d = 2.8R & \delta_m > \delta_p \end{array}\right\} \quad (20)$$

Table 2: *Properties of the tungsten carbide - mild steel impact system*

Material properties
Mild steel slab: $\rho_t = 7850[kg/m^3]$; $E_t = 210[GPa]$; $\nu_t = 0.30[-]$; $S_y = 1.0[GPa]$
Tungsten carbide impactor: $\rho_i = 14500[kg/m^3]$; $E_i = 600[GPa]$; $\nu_i = 0.28[-]$
Other inputs: $m_i = 0.06074[kg]$; $R_i = 10[mm]$; $R_t = \infty$; $V_0 = 0.25[m/s]$

The material properties of the tungsten carbide – mild steel impact system are shown in Table 2. A check using the energy balance algorithm [6] confirmed that the maximum indentation for this impact event is located in the nonlinear elastoplastic loading stage. Hence, the impact stages involved include: elastic loading, nonlinear elastoplastic loading and elastic unloading; all of which are modelled with nonlinear Meyer type compliance models (see equations (19a, b, and e)). Consequently, the FILM solution for the response of a half-space impact

modelled using a general Meyer type contact model (see equations (13, 14, and 16 - 18)) can be applied to all of these impact stages, as will be shown next.

Elastic loading response

Based on equation (19a), $\delta_0 = 0;\ F_0 = 0;\ K_c = K_h;\ q = 3/2;$ and $\delta_n = \delta_y$. From the FILM solution, the following apply to the elastic loading response.

$F_{rs} = K_{rs}(\delta_{rs} - \delta_r) + K_h\delta_r^{3/2}; \qquad K_{rs} = nK_h\delta_y^{1/2}\left[(s/n)^{3/2} - (r/n)^{3/2}\right]; \qquad \delta_r = r\delta_y/n;$

$C_{rs} = \left(K_{rs}\delta_r - K_h\delta_r^{3/2}\right)/K_{rs}.$

Nonlinear elastoplastic loading response

Based on equation (19b), $\delta_0 = \delta_y;\ F_0 = F_y = K_h\delta_y^{3/2};\ K_c = K_h;\ q = 3/2;$ and $\delta_n = \delta_m$. From the FILM solution, the following apply to the nonlinear elastoplastic loading response.

$F_{rs} = K_{rs}(\delta_{rs} - \delta_r) + K_h\left(\delta_r - \delta_y\right)^{3/2} + F_y;$

$K_{rs} = nK_h\left(\delta_m - \delta_y\right)^{1/2}\left[(s/n)^{3/2} - (r/n)^{3/2}\right];$

$\delta_r = \delta_y + r\left(\delta_m - \delta_y\right)/n;$ and $C_{rs} = \left(K_{rs}\delta_r - K_h\left(\delta_r - \delta_y\right)^{3/2} - F_y\right)/K_{rs}.$

The nonlinear elastoplastic loading response covers the indentation range $\delta_y \le \delta \le \delta_m$. Hence, the maximum indentation, δ_m, is determined in this loading stage and can be calculated using the energy-balance algorithm of [6]. Using this algorithm the maximum indentation for the present impact event is estimated from:

$$\frac{1}{2}mV_0^2 = 0.4K_h\delta_y^{5/2} + 0.4K_h\left(\delta_m - \delta_y\right)^{5/2} + K_h\delta_y^{3/2}\left(\delta_m - \delta_y\right) \qquad (21)$$

Unloading response

The unloading response covers the indentation range $\delta_f \le \delta \le \delta_m$. Based on equation (19e) $\delta_0 = \delta_f;\ F_0 = 0;\ K_c = K_u;\ q = 3/2;$ and $\delta_n = \delta_m$. From the FILM solution, the following changes apply to the unloading response.

$F_{rs} = K_{rs}(\delta_{rs} - \delta_r) + K_u\left(\delta_r - \delta_f\right)^{3/2};$

$K_{rs} = nK_u\left(\delta_m - \delta_f\right)^{1/2}\left[(s/n)^{3/2} - (r/n)^{3/2}\right]$;

$\delta_r = \delta_f + r\left(\delta_m - \delta_f\right)/n$; and $C_{rs} = \left(K_{rs}\delta_r - K_u\left(\delta_r - \delta_f\right)^{3/2}\right)/K_{rs}$.

Note that the unloading response has been discretised from the bottom-up, which is why the onset is at the point $\left(\delta_f, 0\right)$ instead of (δ_m, F_m) as might be expected. The bottom-up discretisation has been used for mathematical convenience and gives the same results as would have been obtained if the discretisation was performed from the top-down with the onset at (δ_m, F_m). Additionally, the sign change of the middle term in equation (18) during unloading makes the bottom-up solution consistent with the top-down solution.

The above procedure of the FILM based on the contact model of Big-Alabo *et al* [6] was implemented in a customised *Mathematica*™ code to make independent predictions for the impact response of the tungsten carbide – mild steel impact system. The code was run using five discretisations in each of the impact stages and the closed-form solutions derived for each discretisation were used to extract data points for plotting of the impact histories. Figure 2 shows the results of the FILM approach compared with results obtained by direct numerical integration of the governing nonlinear ODEs for each impact stage; both results are in agreement. The numerical integration results were obtained by solving equation (8) and equations (19a, b, and e) together, using the NDSolve function in Mathematica™. In Figure 2, the blue lines represent the elastic response, the green lines represent the elastoplastic response, and the black lines represent the unloading response. This colour definition is used in subsequent figures, where applicable.

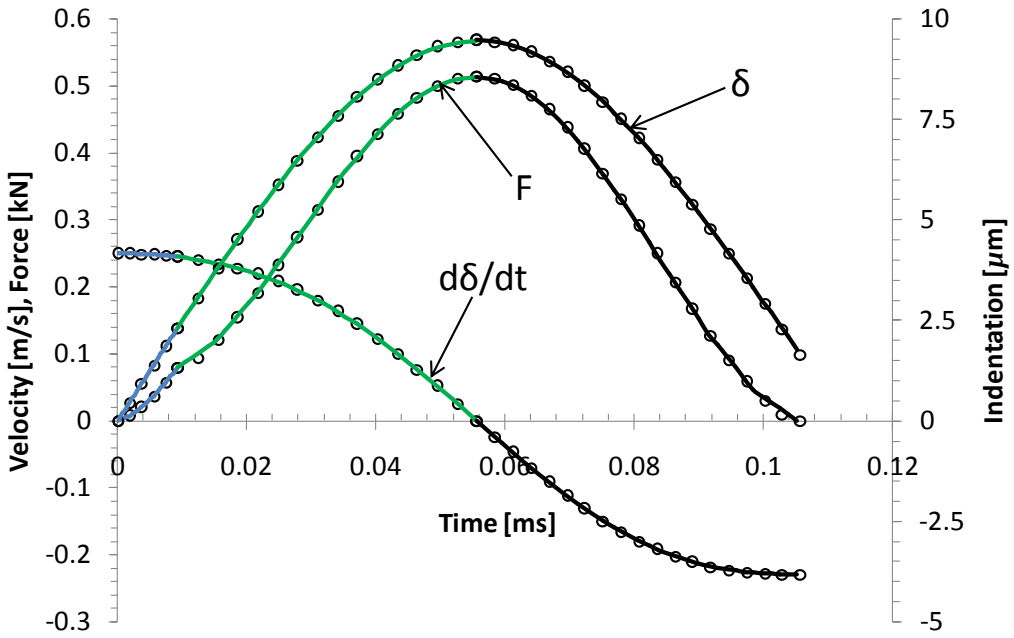

Figure 2: *Elastoplastic impact response of tungsten-carbide - mild steel impact system. Lines - FILM solution; Markers - numerical solution. Contact model used: Big-Alabo et al [6].*

3.2. Solution of half-space impact modelled based on a non-Meyer type contact model using the FILM

In this section, the generalised FILM approach derived in Section 2 is applied to demonstrate how the response of a half-space impact stage modelled using a non-Meyer type contact model can be determined. Non-Meyer type contact models are contact models that cannot be expressed in terms of equation (1) or (9); examples include the elastoplastic loading models of Stronge [4] and Brake [5]. Experience indicates that conventional numerical integration schemes do not guarantee convergent solutions for half-space impact models in which non-Meyer type contact models are used to estimate the impact force [11]. This does not mean that impact models incorporating non-Meyer type contact models cannot be solved numerically, but that they are more challenging to solve because in some cases a numerical solution may not be found, see for example [11]. In contrast, the

FILM guarantees convergent solutions for half-space impact models incorporating non-Meyer type contact models, and produces the solution with the same relative ease as for half-space impact models incorporating Meyer type contact models. This is because the FILM uses closed-form solutions that do not diverge or oscillate, and the number of discretisations need not be increased to guarantee convergent solutions even when a more complex contact model is used to estimate the impact force. To demonstrate this, the FILM is used to solve the tungsten-carbide impact problem discussed in section 3.1 when the non-Meyer type contact model of Stronge [4] is used to estimate the impact force.

For details of Stronge's contact model, the reader is referred to reference [4]. In Stronge's contact model the elastic loading stage is modelled using the Hertz compliance model (see equation (19a)), while the model for the elastoplastic loading stage uses a logarithmic function of indentation depth, see equation (2). The model for the unloading stage is the same as equation (19e), the only difference being the expression for R_d. Stronge [4] estimated the deformed effective radius as $R_d = \left(2\delta_m/\delta_y - 1\right)R$. All three stages are modelled using nonlinear compliance models and therefore, the corresponding impact models require numerical solution. In the following analysis, the FILM approach is applied to determine the impact histories while using Stronge's contact model to estimate the impact response. Note that the compliance models for both the elastic loading and the unloading stages are Meyer type models and the solution for the response of the corresponding impact stages, obtained using the FILM, are derived in Section 3.1. It is only the elastoplastic loading stage that is predicted with a non-Meyer type compliance model. This is also the case with other non-Meyer type contact models [5, 9, 10].

Elastic loading response

The FILM solution for the elastic loading stage of the impact response is the same as in Section 3.1, since Stronge [4] also used the Hertz model to estimate the elastic impact response.

Nonlinear elastoplastic loading response

Using equations (2) and (8), the elastoplastic impact response based on Stronge's model is given as:

$$m\ddot{\delta} + F_y\left(\frac{2\delta}{\delta_y} - 1\right)\left[1 + \frac{1}{3.3} ln\left(\frac{2\delta}{\delta_y} - 1\right)\right] = 0 \tag{22}$$

Obviously, equation (22) is quite a complex nonlinear ODE and ordinarily would require solution via conventional numerical means. Instead, in this section the FILM is used to determine the impact response. For the elastoplastic impact event considered here, the nonlinear elastoplastic loading response covers the indentation range $\delta_y \leq \delta \leq \delta_m$. Again, the maximum indentation, δ_m, is estimated using the energy-balance principle. Using equation (2), Stronge [4] derived the indentation work from the beginning of the elastic loading to any point in the elastoplastic loading stage as:

$$W = W_y\left\{0.47 + 0.53\left(\frac{2\delta}{\delta_y} - 1\right)^2 + 0.189\left(\frac{2\delta}{\delta_y} - 1\right)^2 ln\left(\frac{2\delta}{\delta_y} - 1\right)\right\} \tag{23}$$

where $W_y = 0.4K_h\delta_y^{5/2}$. Therefore, the maximum indentation of an elastoplastic impact can be determined based on Stronge's model by equating the deformation work in equation (23) to the initial impact energy as follows:

$$\frac{1}{2}mV_0^2 = W_y\left\{0.47 + 0.53\left(\frac{2\delta_m}{\delta_y} - 1\right)^2 + 0.189\left(\frac{2\delta_m}{\delta_y} - 1\right)^2 ln\left(\frac{2\delta_m}{\delta_y} - 1\right)\right\} \tag{24}$$

Based on Stronge's elastoplastic model, $\delta_0 = \delta_y$; $F_0 = F_y = K_h\delta_y^{3/2}$; and $\delta_n = \delta_m$.

Using equations (5) to (8) and (2), the linearised model for each discretisation of the elastoplastic response is derived as:

$$m\ddot{\delta}_{rs} + K_{rs}\delta_{rs} = K_{rs}\delta_r - F_y\left(\frac{2\delta_r}{\delta_y} - 1\right)\left[1 + \frac{1}{3.3}ln\left(\frac{2\delta_r}{\delta_y} - 1\right)\right] \quad (25)$$

where $F_{rs} = K_{rs}(\delta_{rs} - \delta_r) + F_y\left(\frac{2\delta_r}{\delta_y} - 1\right)\left[1 + \frac{1}{3.3}ln\left(\frac{2\delta_r}{\delta_y} - 1\right)\right]$;

$K_{rs} = 2K_h\delta_y^{1/2}\left\{1 + \frac{n}{6.6}\left[\left(\frac{2\delta_s - \delta_y}{\delta_m - \delta_y}\right)ln\left(\frac{2\delta_s - \delta_y}{\delta_y}\right) - \left(\frac{2\delta_r - \delta_y}{\delta_m - \delta_y}\right)ln\left(\frac{2\delta_r - \delta_y}{\delta_y}\right)\right]\right\}$; and

$\delta_r = \delta_y + r(\delta_m - \delta_y)/n.$

The solution to equation (25) can be expressed as equations (16) to (18) with

$C_{rs} = \frac{1}{K_{rs}}\left\{K_{rs}\delta_r - F_y\left(\frac{2\delta_r}{\delta_y} - 1\right)\left[1 + \frac{1}{3.3}ln\left(\frac{2\delta_r}{\delta_y} - 1\right)\right]\right\}.$

Note that the derivation of the FILM solution for this elastoplastic loading stage is made possible because of the general form in which the FILM has been formulated in Section 2.

Application of FILM solution to the unloading response

Since Stronge's model for the unloading stage is the same as equation (19e) the FILM solution for the unloading response in section 3.1 is applicable here.

The above procedure of the FILM, derived for the various impact stages modelled using Stronge's contact model, was implemented in a customised *Mathematica*™ code that was used to estimate the impact response of the tungsten carbide – mild steel impact event. The code was run using five discretisations in each of the impact stages and the closed-form solutions derived for each discretisation were used to extract data points for plotting the impact histories. Figure 3 shows the results of the FILM approach in comparison with results obtained by direct numerical integration using the NDSolve function. Again, the results of both methods are in agreement.

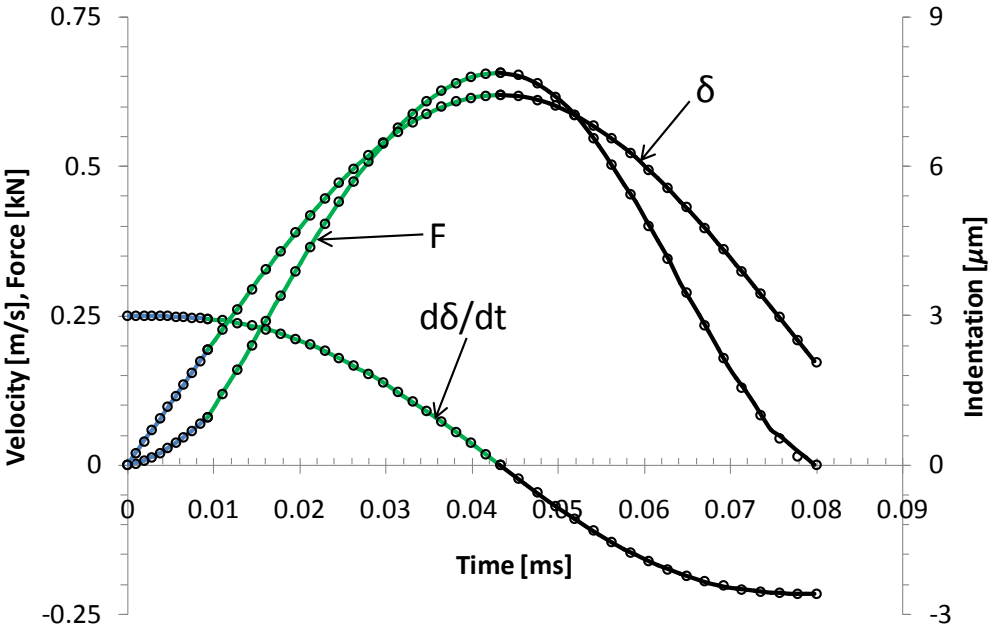

Figure 3: *Comparison of the results of the FILM solution and numerical integration method. Lines - FILM solution; Markers - numerical solution. Contact model used: Stronge [4].*

Table 3: *Tungsten carbide - mild steel response results obtained using FILM*

Impact parameters	Results	
	Model of Big-Alabo *et al* [6]	**Stronge's model [4]**
Impact duration [μs]	105.14	79.78
Time at maximum indentation [μs]	55.57	43.24
Permanent indentation [μm]	1.78	2.09
Maximum indentation [μm]	9.45	7.44
Maximum impact force [N]	513.41	657.29
Final rebound velocity [m/s]	0.23	0.22
Coefficient of restitution [-]	0.92	0.87

A comparison of the estimates of some critical impact parameters estimated based on the contact models of Big-Alabo *et al* [6] and Stronge [4] is presented in Table 3. The results reveal that the contact model used to estimate the impact force can greatly influence the predictions of a half-space impact response. Given that the contact model of Big-Alabo *et al* [6] was found to predict experimental measurements of tungsten carbide sphere indenting a steel half-space better than

Stronge's contact model [5, 6], this suggests that the impact response predicted using the contact model of Big-Alabo *et al* [6] is more reliable.

4. Solution of the response of an infinite plate impact using the FILM approach

During normal impact of transversely inflexible plates, which can be modelled using half-space assumptions, the flexural oscillations are negligible. The impact energy is primarily used for local indentation of the plate. The implication is that the impactor velocity is zero at maximum indentation, which also marks the end of the impact loading. These features of a half-space impact allow for the use of the energy-balance principle in estimating the maximum indentation during impact loading [16]. For normal impact of a transversely flexible plate the flexural oscillations of the plate cannot be neglected, and the interactions between the flexural oscillations and the local indentation determine the impact response. The response is dynamic and complex, making it impossible to use the energy-balance principle to determine the maximum indentation for a transversely flexible plate impact [16].

In order to determine the complete impact response using the FILM the indentation and impact force at the end of the loading must be known. The end conditions of the impact loading are used as the initial conditions for the unloading response. While it is possible to have this information from the energy-balance principle in the case of a transversely inflexible plate impact, it is not possible in the case of a transversely flexible plate impact. However, the impact loading during a transversely flexible plate impact ends when the impactor velocity is zero because the impact loading is due to the deceleration of the impactor. If the end indentation of the impact loading is chosen in advance, such that this assumed end indentation is definitely higher than the actual end indentation, then the condition

of zero impactor velocity can be used as a test condition to determine the actual end of the impact loading. In principle the maximum indentation of the corresponding elastic half-space impact is always greater that the actual end indentation of the transversely flexible plate impact and this can therefore be conveniently used as the assumed end indentation.

The maximum indentation of a transversely flexible plate impact occurs when the relative velocity of the impactor and the plate is zero. For impact events in which the impact force history does not oscillate, the condition of zero relative velocity occurs only once and this is at the maximum indentation point. Hence, the zero relative velocity condition is sufficient to determine the point where the maximum indentation occurs when the impact force history does not oscillate. This does not mean that the zero relative velocity condition can be used to determine the maximum indentation in order to implement the FILM approach. Rather, the zero relative velocity condition can only be used as a test condition during implementation of the FILM approach to know when the maximum indentation is reached. The infinite plate impact is an example of a transversely flexible plate impact characterised by a non-oscillating impact force history, and its response can therefore be determined using the FILM.

In cases where the impact force history oscillates, the zero relative velocity condition occurs more than once, making it necessary to have another condition to determine the maximum indentation point. Apparently, such a complementary condition is not known. Hence, the zero relative velocity condition is not sufficient to determine the maximum indentation when the impact force history oscillates. The oscillation of the impact force history is due to the influence of vibration waves reflected from the boundary. Thus, the FILM approach is more difficult to implement for a transversely flexible plate impact with an oscillating impact force

history, and for such cases, a suitable conventional numerical method should be used. Therefore, the FILM is recommended only for transversely flexible plate impacts with non-oscillatory impact force history e.g. infinite plate impacts.

By definition, the infinite plate impact is a transversely flexible plate impact in which the influence of the boundary conditions on the impact response is negligible. Hence, the infinite plate impact is characterised by a non-oscillating impact force history since oscillations in the impact force history arise due to the influence of boundary conditions. As explained above the FILM can be used to solve the nonlinear ODE of an infinite plate impact with slight modifications. To demonstrate this, an elastic impact problem studied by Olsson [26] is re-examined here. The material and geometrical properties of the graphite/epoxy composite laminate plate and steel impactor used by Olsson [26] are given in Table 4. The infinite plate model for an orthotropic composite plate is a single ordinary differential equation given by [26]:

$$\ddot{\delta} + \frac{1}{8\sqrt{\rho D}}\dot{F} + \frac{F}{m} = 0 \tag{26}$$

where ρ is the mass per unit area of the plate [kg/m^2], D is the effective mechanical bending stiffness of the plate [Nm], m is the mass of the impactor [kg] and F is the impact force [N]. The effective stiffness is calculated as $D = [(A + 1)/2]\sqrt{D_{11}D_{22}}$ where $A = (D_{12} + 2D_{66})/\sqrt{D_{11}D_{22}}$. The D_{ij} constants are bending stiffness constants that are calculated from the material properties of the plate. Note that the theoretical model for the coaxial impact of a spherical mass and a dome-ended slender rod is provided in the form of equation (26) [2, 4].Hence, the FILM solution for equation (26) can be applied to the sphere-rod coaxial impact problem.

Table 4: *Properties of the steel – laminate plate impact system [26]*

Material properties
Graphite/epoxy (T300/934) plate: Lamination sequence = $[0/90/0/90/0]_s$; $\rho = 4.132\ [kg/m^2]$; $D_{11} = 154.9\ [Nm]$; $D_{12} = 4.76\ [Nm]$; $D_{22} = 91.4\ [Nm]$; $D_{66} = 8.97\ [Nm]$; $h = 2.69\ [mm]$; $A = 200 \times 200\ [mm^2]$;
Impactor (Steel): $m = 8.3\ [g]$; $V_0 = 3\ [m/s]$; $R_i = 6.35\ [mm]$
Other inputs: Effective contact modulus $= 9.72\ [GPa]$; $R_t = \infty$

The impact force in equation (26) can be estimated using a static contact model and is a function of the local indentation i.e. $F = F(\delta)$. Hence, substituting an appropriate static contact model in equation (26) would produce a differential equation in $\delta(t)$, the solution of which gives the local indentation history. The local indentation is expressed as: $\delta(t) = w_i(t) - w(t)$ where $w_i(t)$ and $w(t)$ are respectively the displacements of the impactor and the plate at the point of impact. The displacement of the plate at the point of impact is given by:

$$w(t) = \frac{1}{8\sqrt{\rho D}} \int_{t_0}^{t} F(\tau)\, d\tau \tag{27}$$

where t_0 is the time at the onset of the impact stage considered, and $t_0 = 0$ for elastic impact.

The complete solution of the infinite plate impact model can be determined once the local indentation history is obtained from the solution of equation (26). The local indentation history is used to determine the impact force history from the static contact model that was initially substituted into equation (26), and the impact force so obtained is substituted into equation (27) to determine the displacement of the plate at the point of impact. Thereafter, the displacement of the impactor can be obtained from the solutions of the local indentation and plate displacement. Also, the velocities of the impactor and the plate can be obtained by differentiating the solutions of the respective displacements.

During elastic impact of transversely flexible composite plates, the Hertz contact model (a specific Meyer type contact model – see Section 3.1) can be used to estimate the impact force. Substituting the Hertz contact model in equation (26) the model for the elastic response of an infinite plate impact is derived thus:

$$\ddot{\delta} + \frac{3K_h}{16\sqrt{\rho D}}\delta^{1/2}\dot{\delta} + \frac{K_h}{m}\delta^{3/2} = 0 \tag{28}$$

The initial conditions are $\delta(0) = 0$ and $\dot{\delta}(0) = V_0$. Equation (28) is a nonlinear differential equation and would normally require solution using numerical means, and depending on the numerical algorithm used, the solution may sometimes fail to converge or produce accurate results. Using the FILM, by substituting the linearised contact force from discretisation of Hertz contact model (see section 3.1) into equation (26), the impact response model for each discretisation is:

$$\ddot{\delta}_{rs} + \frac{K_{rs}}{8\sqrt{\rho D}}\dot{\delta}_{rs} + \frac{K_{rs}}{m}\delta_{rs} = \frac{K_{rs}\delta_r - K_h\delta_r^{3/2}}{m} \tag{29}$$

where $K_{rs} = nK_h\delta_m^{1/2}\left[(s/n)^{3/2} - (r/n)^{3/2}\right]$; $\delta_r = r\delta_m/n$; $r = 0, 1, 2, 3, \ldots, n-1$; $s = r + 1$; and n is the number of discretisations. Since the maximum indentation of the infinite plate model cannot be determined from the onset as explained above, the maximum indentation of the corresponding elastic half-space impact is used and the zero relative velocity condition is tested for each linearisation to determine the point when the actual maximum indentation is reached. This maximum indentation is less than that of the corresponding elastic half-space impact [26]. However, the impact loading ends when the impactor velocity is zero. This second condition is also tested to determine the end of the impact loading and to determine the initial conditions at the beginning of the unloading stage.

Equation (29) can be rewritten as

$$\ddot{\delta}_{rs} + 2\lambda_{rs}\omega_{rs}\dot{\delta}_{rs} + \omega_{rs}^2\delta_{rs} = P_{rs} \tag{30}$$

where $\lambda_{rs} = (1/16)\sqrt{mK_{rs}/\rho D}$; $\omega_{rs} = \sqrt{K_{rs}/m}$; and $P_{rs} = \left(K_{rs}\delta_r - K_h\delta_r^{3/2}\right)/m$ are the damping constant, circular frequency and load of the linearised response, respectively. Equation (30) describes the response of an initially excited damped oscillator with a constant load. The solution depends on the value of the damping constant, λ_{rs}, i.e. whether the response is under-damped, critically-damped or over-damped. The complete solutions to equation (30) are comprised of the particular and homogeneous solutions for the different cases of damping and are given as:

Under-damped $(0 < \lambda_{rs} < 1)$

$$\delta_{rs} = R_{rs}e^{-\lambda_{rs}\omega_{rs}t}\,\mathrm{Sin}(\omega_{drs}t + \varphi_{drs}) + C_{rs} \tag{31}$$

Critically-damped $(\lambda_{rs} = 1)$

$$\delta_{rs} = e^{-\omega_{rs}t}\,[A_{rs} + B_{rs}t] + C_{rs} \tag{32}$$

Over-damped $(\lambda_{rs} > 1)$

$$\delta_{rs} = e^{-\lambda_{rs}\omega_{rs}t}\left[D_{rs}e^{\left(\lambda_{rs}^2-1\right)^{1/2}\omega_{rs}t} + E_{rs}e^{-\left(\lambda_{rs}^2-1\right)^{1/2}\omega_{rs}t}\right] + C_{rs} \tag{33}$$

where $\omega_{drs} = \omega_{rs}\sqrt{1-\lambda_{rs}^2}$ is the damped circular frequency of the under-damped response;

$R_{rs} = e^{\lambda_{rs}\omega_{rs}t_r}\left[\left(\dot{\delta}_r + \lambda_{rs}\omega_{rs}(\delta_r - C_{rs})\right)^2/\omega_{drs}^2 + (\delta_r - C_{rs})^2\right]^{1/2}$ is an initial-value constant that determines the amplitude of the homogeneous solution for the under-damped response;

$\varphi_{drs} = \tan^{-1}\left[\omega_{drs}(\delta_r - C_{rs})/\left(\dot{\delta}_r + \lambda_{rs}\omega_{rs}(\delta_r - C_{rs})\right)\right] - \omega_{drs}t_r$ is the phase angle of the homogeneous solution for the under-damped response;

$A_{rs} = \left[-\dot{\delta}_r t_r + (\delta_r - C_{rs})(1 - \omega_{rs}t_r)\right]e^{\omega_{rs}t_r}$ and $B_{rs} = \left[\dot{\delta}_r + \omega_{rs}(\delta_r - C_{rs})\right]e^{\omega_{rs}t_r}$ are initial-value constants of the critically-damped response;

$D_{rs} = \left[\frac{\omega_{rs}(\delta_r - C_{rs})\left(\lambda_{rs} + \left(\lambda_{rs}^2-1\right)^{1/2}\right) + \dot{\delta}_r}{2\omega_{rs}\left(\lambda_{rs}^2-1\right)^{1/2}}\right]e^{\left[\lambda_{rs} - \left(\lambda_{rs}^2-1\right)^{1/2}\right]\omega_{rs}t_r}$ and

$E_{rs} = \left[\frac{\omega_{rs}(\delta_r - C_{rs})\left(-\lambda_{rs} + (\lambda_{rs}^2 - 1)^{1/2}\right) - \dot{\delta}_r}{2\omega_{rs}(\lambda_{rs}^2 - 1)^{1/2}}\right] e^{\left[\lambda_{rs} + (\lambda_{rs}^2 - 1)^{1/2}\right]\omega_{rs} t_r}$ are initial-value constants of the over-damped response; and

$C_{rs} = P_{rs}/\omega_{rs}^2 = \left(K_{rs}\delta_r - K_h\delta_r^{3/2}\right)/K_{rs}$ is the particular solution.

Evaluation of the solutions, see equations (31 – 33), depend on the initial conditions, i.e. $\delta(t_r) = \delta_r$ and $\dot{\delta}(t_r) = \dot{\delta}_r$. Since the indentation at the boundaries of each discretisation, δ_r, is known, then the time at the boundaries of each discretisation, t_r, can be determined by substituting $\delta_{rs} = \delta_r$ when $t = t_r$ in equations (31 – 33). Closed-form solutions for t_r cannot be obtained from the resulting nonlinear equations and so t_r is determined using conventional numerical methods for finding roots of nonlinear equations e.g. the Newton-Raphson method. Therefore, the application of the FILM to solve the infinite plate impact model is semi-analytical since the time at the boundaries must be obtained from an implicit formulation. This is in contrast to half-space impacts where the time at the boundaries is obtained from an explicit formulation and the FILM is completely analytical.

The above procedure of the FILM, derived for elastic response of an infinite plate impact, was developed into a customised code that was used to solve the elastic impact response of the steel – composite laminate impact mentioned above. Results obtained from the FILM, and also via direct numerical integration of equation (28) using the NDSolve function, are plotted in Figure 4. Both results are in agreement and this shows that the FILM solution is accurate. Olsson [26] determined the force-time response for this example by numerically integrating the normalised form of equation (28). From the force-time plot, the maximum impact force and time duration are approximately 270.0 [*N*] and 245.0 [*μs*] respectively. The FILM approach gives corresponding results of 303.3 [*N*] and 261.1

[μs], whereas numerical integration using the NDSolve function gives 302.6 [N] and 262.6 [μs]. Since the FILM and NDSolve solutions are in agreement and differ significantly from Olsson's solution, this suggests that Olsson's solution did not accurately converge; an observation that underscores the need for independent verification of numerical results even when a convergent numerical solution is obtained. The FILM can be used to fulfil this purpose.

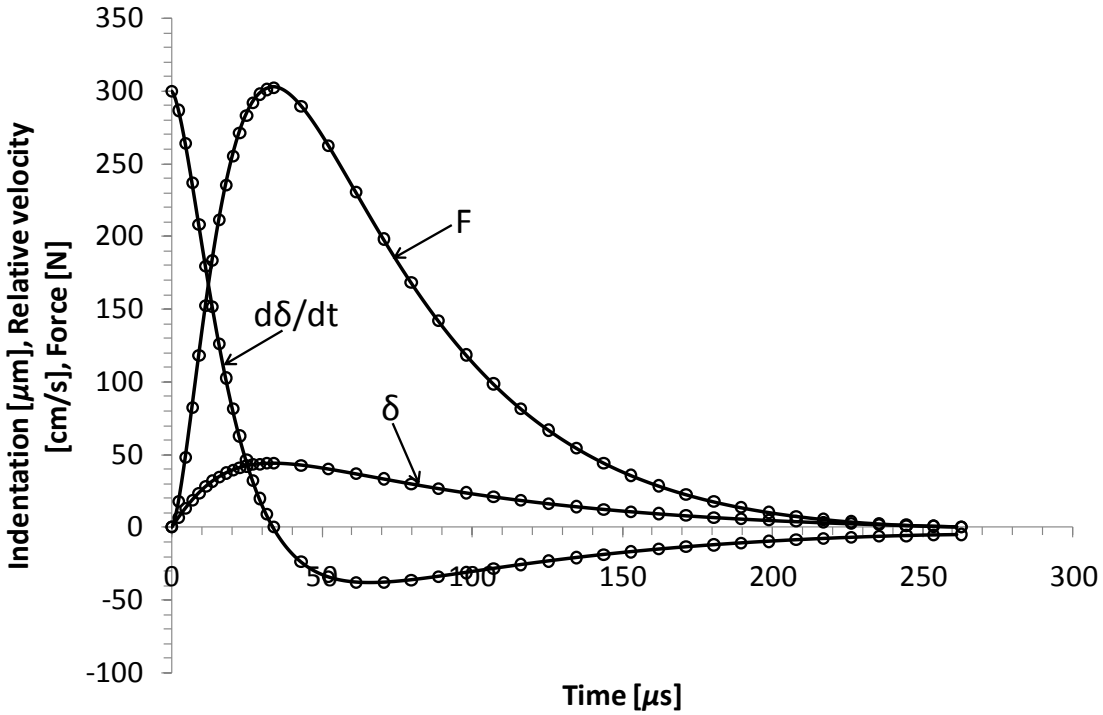

Figure 4: *Comparison of the results of the FILM solution and numerical integration method for elastic impact of $[0/90/0/90/0]_s$ graphite/epoxy (T300/934) composite plate. Lines – FILM solution; Markers – numerical solution.*

Since the time boundaries of the FILM solution for infinite plate response are determined numerically, much more than five discretisations is required to obtain accurate results. In simulating the FILM solution for the response of the steel – composite laminate impact, $n = 50$ was used for descritisation of the assumed maximum indentation to ensure that accurate results were obtained. The zero relative velocity condition was satisfied at the 23rd discretisation. The actual maximum indentation obtained was 44.2 [μm] while the corresponding half-space

maximum indentation used for the discretisation was calculated as 96.0 [μm]. Once the actual maximum indentation was reached, the restitution algorithm of the FILM was used with $n = 20$ to obtain the response from this maximum indentation to the end of the impact where the impact force is zero. Normally the restitution algorithm of the FILM should be applied at the end of the impact loading when the impactor velocity is zero. But in the present simulation it was applied at the point of maximum indentation to simplify the computations required in achieving the solution provided by the FILM; this did not affect the results because the model for loading and restitution are the same for elastic impact.

The infinite plate impact response is characterised by a monotonic increase in indentation from the beginning of the impact response to the point of maximum indentation, and afterwards, it decreases monotonically until the end of the impact response. Therefore, in applying the FILM to determine the response of an infinite plate impact, the FILM solution for the last impact loading stage is applied until the maximum indentation is reached i.e. when the relative velocity is zero. Thereafter, the restitution algorithm of the FILM, which is based on the compliance model for the last loading stage, is applied until the end of the impact loading is reached i.e. when the impactor velocity is zero. From the point of the end of the impact loading, the restitution algorithm of the FILM, which is based on the restitution compliance model, is applied until the end of the impact response where the impact force is zero.

Although the application of the FILM to the infinite plate model requires many discretisations to guarantee accurate results, the stability of the approach is independent of the number of discretisation i.e. the FILM is stable with few discretisations, such as $n = 10$ (see Figures 5 and 6). The implication of the unconditional stability of the FILM is that convergent solutions can always be

obtained for the infinite plate problem irrespective of the contact model used to estimate the impact force.

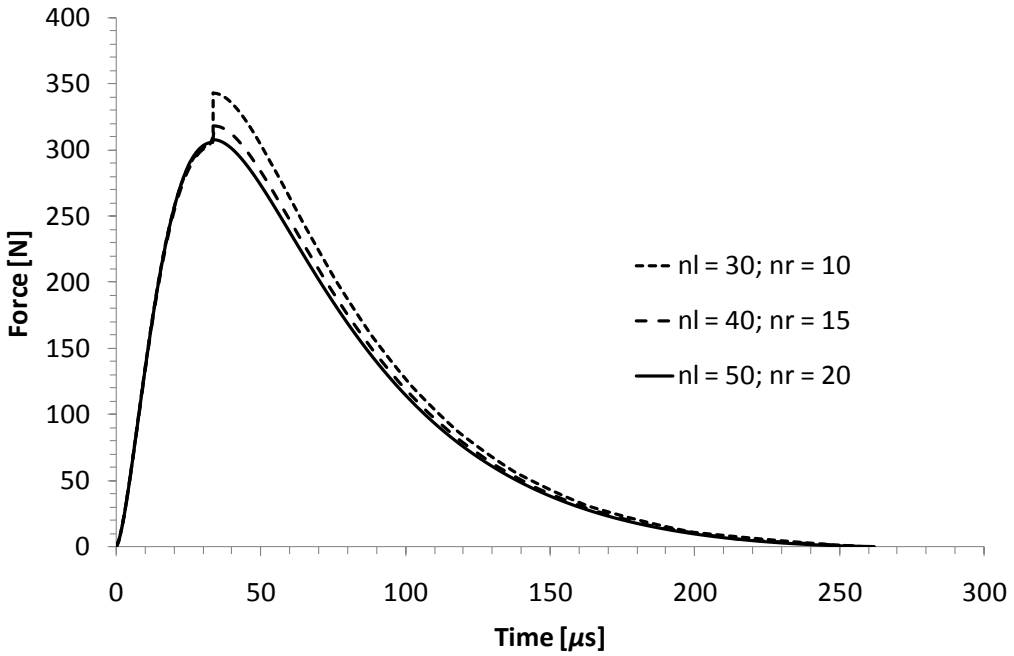

Figure 5: *Convergence test for FILM solution of infinite plate impact response. nl = initial discretisation used to determine maximum point; nr = number of discretisation used from maximum point to end of impact.*

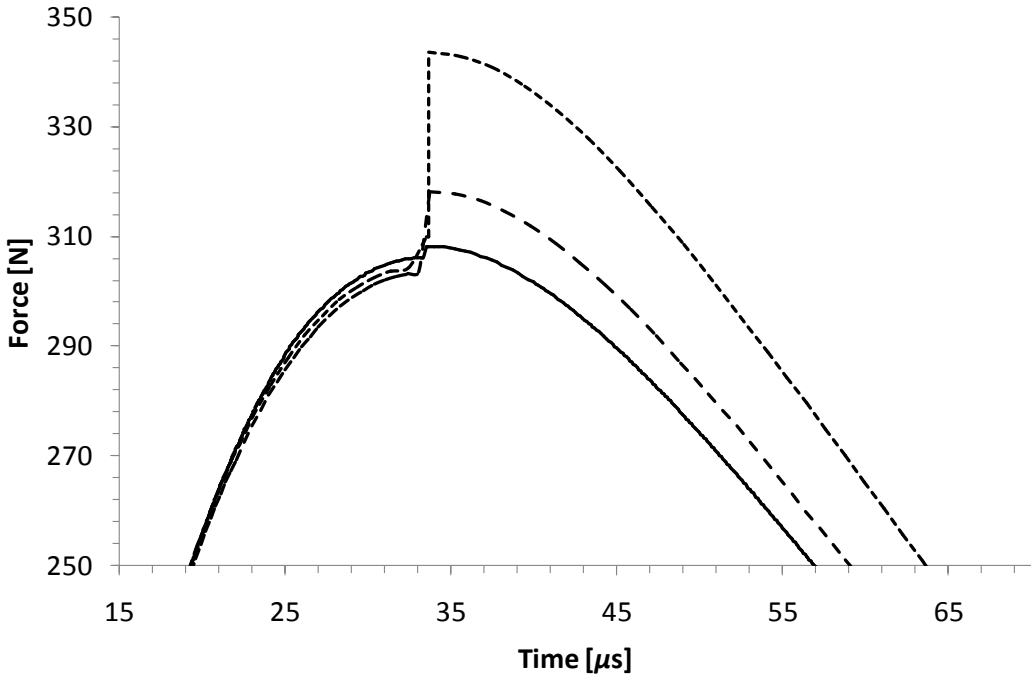

Figure 6: *Exploded view of the peak response area of Figure 5.*

In the example just considered, the FILM solution was derived for an infinite plate impact event in which the impact force was estimated using a specific Meyer type contact model, i.e. the Hertz elastic contact model. In addition, the compliance model for the impact loading stage was the same as that of the unloading stage. This case study was used to demonstrate the formulation of the FILM solution for infinite plate impact. Nevertheless, the FILM solution for the infinite plate impact derived above can also be shown to be applicable even when a non-Meyer type contact model is used to estimate the impact force of an impact stage, and when different nonlinear compliance models are used to estimate the various impact stages involved. For such cases, equations (5 - 7) are used to make the necessary changes in the constants P_{rs}, K_{rs} and δ_r, for each of the impact stages involved. During the impact loading phase, the test conditions for the point of maximum indentation and the end point of the impact loading are implemented in the last impact loading stage. For example, the test conditions are implemented in the second loading stage of an impact response involving two loading stages. The details of the end conditions are then used to determine the initial conditions of the unloading response.

5. Conclusions

Asymptotic impact conditions are used to simplify the analytical models for investigating the response of certain impact events. Asymptotic impact events are modelled using single differential equations [16]. Three asymptotic impact conditions are generally identified in the literature, namely: half-space impact, infinite plate impact and quasi-static bending impact. These three asymptotic cases are used to model and analyse a wide range of typical impact events and to

design impact experiments. Hence, the solution to the asymptotic impact models, which are realistically expressed in the form of nonlinear ODEs, is important.

Half-space and infinite plate impacts are normally characterised by significant local indentation and these impact events have been referred to here as asymptotic impacts with significant local indentation. This paper deals with the solution of nonlinear models of asymptotic impacts involving significant local indentation, using the FILM approach. A novel and powerful solution algorithm, the *Force Indentation Linearised Method* (FILM), first introduced in reference [18], was reformulated in a more general form in section 2. This general formulation of the FILM enabled solutions to be found, even when non-Meyer type contact models were used to estimate the impact response. Solutions derived for half-space and infinite plate impacts were used as case studies to demonstrate the novel method; detailing how the FILM could be implemented to solve asymptotic impact events with significant local indentation. Results of the FILM solution were validated using results obtained from conventional numerical integration. It was shown that the FILM could solve the considered nonlinear impact models with the same relative ease irrespective of the complexity of the nonlinearity in the contact model used to estimate the impact force.

The FILM algorithm for half-space impact does not oscillate or diverge and is therefore inherently stable. The implication is that the FILM algorithm will always converge to a solution, making it a preferable choice to the conventional numerical methods that are conditionally stable. The accuracy of the results obtained using the FILM depends on the number of discretisation used; which in turn determines the computational effort. For half-space impacts, the FILM is completely analytical and accurate solutions can be obtained with only a few discretisation of the nonlinear compliance model; typically five to ten. This means

that the results obtained using the FILM can be verified by hand calculation. For infinite plate impacts, the FILM is semi-analytical and compared to half-space impacts, requires more discretisation to obtain accurate results.

Advantages of the FILM algorithm are its simplicity, inherent stability and rapid convergence. Perhaps its main advantage lies in its ability to solve the nonlinear model of an asymptotic impact involving significant local indentation with the same relative ease, irrespective of whether the impact force is estimated using a Meyer type or non-Meyer type contact model. This makes the FILM an interesting algorithm for implementation in commercial finite element software, such as ABAQUS. The result would be a robust and efficient algorithm for impact analysis. This implementation will be a goal for future research.

Acknowledgement

The first author is grateful to the Commonwealth Scholarship Commission (CSC), UK for funding his PhD research (CSC Award Ref: NGCA-2011-60), of which this work is a part.

References

[1] Johnson KL. Contact Mechanics, *Cambridge University Press*, Cambridge, 1985.

[2] Goldsmith W. Impact: The Theory and Physical Behaviour of Colliding Solids, *Dover Publications*, New York, 2001.

[3] Yigit AS and Christoforou AP. On the Impact of a Spherical Indenter and an Elastic-Plastic Isotropic Half-Space, *Composite Engineering*, 1994; 4 (11), pp 1143 – 1152.

[4] Stronge WJ. Impact Mechanics, *Cambridge University Press*, Cambridge, 2000.

[5] Brake MR. An Analytical Elastic-Perfectly Plastic Contact Model, *International Journal of Solids and Structures*, 2012; 49, pp 3129 – 3141.

[6] Big-Alabo A, Harrison P, Cartmell MP. Contact Model for Elastoplastic Analysis of Half-space Indentation by a Spherical Impactor, *Computers and Structures*, 2015; 151, pp 20 – 29.

[7] Cairns DS. A Simple, Elasto-Plastic Contact Law for Composites, *Journal of Reinforced Plastics and Composites*, 1991; 10, pp 423 – 433.

[8] Majeed MA, Yigit AS, Christoforou AP. Elastoplastic Contact/Impact of Rigidly Supported Composites, *Composites: Part B*, 2012; 43, pp 1244 – 1251.

[9] Li LY, Wu CY, Thornton C. A theoretical model for the contact of elastoplastic bodies, *Proc. IMechE, Part C: Journal of Mechanical Engineering Science*, 2002; 216, pp 421 – 431.

[10] Jackson RL and Green I. A Finite Element Study of Elasto-Plastic Hemispherical Contact Against a Rigid Flat, *Journal of Tribology*, 2005; 127, pp 343 – 354.

[11] Big-Alabo A, Harrison P, Cartmell MP. Elastoplastic Half-space Impact Analysis Using a Novel Contact Model that Accounts for Post-yield Effects, *Proceedings*

of the 9th International Conference on Structural Dynamics, EURODYN, Porto, 30 June – 2 July, 2014.

[12] Du, Y. and Wang, S. Energy dissipation in normal elastoplastic impact between two spheres, *Transactions of ASME: Journal of Applied Mechanics*, 2009; 76, 061010-1 – 061010-8.

[13] Christoforou AP and Yigit AS. Effect of Flexibility on Low Velocity Impact Response, *Journal of Sound and Vibration*, 1998; 217 (3), pp 563 – 578.

[14] Yigit AS and Christoforou AP. Limits of Asymptotic Solutions in Low-velocity Impact of Composite Plates, *Composite Structures*, 2007; 81, pp 568 – 574.

[15] Olsson R. Mass Criterion for Wave Controlled Impact Response of Composite Plates, *Composites: Part A*, 2000; 31, pp 879 – 887.

[16] Abrate S. Impact on Composite Structures, *Cambridge University Press*, Cambridge, 1998.

[17] Wolfram Research Inc. Mathematica Version 9.0, *Wolfram Research Inc.*, Champaign, Illinois, 2012.

[18] Big-Alabo A, Harrison P, Cartmell MP. Algorithm for the solution of elastoplastic half-space impact: Force-Indentation Linearisation Method, *Proc. IMechE, Part C: Journal of Mechanical Engineering Sciences*, 2015; 229(5), pp 850 – 858.

[19] Szilard, R. Theory and Applications of Plate Analysis: Classical, Numerical and Engineering Methods, *John Wiley & Sons Inc.*, New Jersey, 2004.

[20] Reddy, JN. Mechanics of Laminated Composite Plates and Shells: Theory and Analysis, 2nd Edition, *CRC Press*, Boca Raton, 2004.

[21] Tillett JPA. A Study of the Impact of Spheres on Plate, *Proceedings of the Physical Society: Section B*, 1954; 67 (9), pp 677 – 688.

[22] Mok CH and Duffy J. The Dynamic Stress-Strain Relation of Metals as Determined from Impact Test with a Hard Ball, *International Journal of Mechanical Sciences*, 1964; 7, pp 355 – 371.

[23] Tabor D. Hardness of Metals, *Oxford University Press*, London, 1951.

[24] Big-Alabo A. Multilayered Sensor-Actuator Plates for Active Mitigation of Elastoplastic Impact Effects, PhD Dissertation, *School of Engineering*, University of Glasgow, UK, 2015.

[25] Big-Alabo A, Harrison P, Cartmell MP. Preliminary Investigations of the Low-Velocity Impact Response of a Smart Trimorph Plate for Active Damage Mitigation, *5th Thematic Conference on Computational Methods in Structural Dynamics and Earthquake Engineering, COMPDYN*, Crete Island, Greece, 25 – 27 May, 2015.

[26] Olsson R. Impact Response of Orthotropic Composite Laminates Predicted by a One-Parameter Differential Equation, *AIAA Journal*, 1992; 30 (6), pp 1587 – 1596.

Nomenclature

m	Mass of impactor/projectile
n	Number of discretisations in the FILM
$w_i(t)$	Displacement of impactor during infinite plate impact
$w(t)$	Displacement of plate during infinite plate impact
D	Effective bending stiffness of an infinite plate
E	Effective contact modulus
F	Contact/impact force
F_m	Maximum contact force
F_p	Contact force at onset of fully plastic loading
F_{rs}	Linearised impact force for discretisation between points r and s
F_{tep}	Contact force at transition point in the elastoplastic loading stage
F_u	Contact force during unloading
F_y	Contact force at yield point
K_h	Hertz contact stiffness
K_c	Contact stiffness
K_l	Linear contact stiffness during elastoplastic loading
K_p	Linear contact stiffness during fully plastic loading
K_{rs}	Linearised contact stiffness for discretisation between points r and s
K_u	Nonlinear contact stiffness during unloading
R	Effective contact radius
R_d	Deformed effective contact radius
S_y	Yield stress
V_0	Initial approach velocity of impactor
δ	Indentation

δ_f Fixed or permanent indentation

δ_m Maximum indentation

δ_p Indentation at the onset of fully plastic loading

δ_r Indentation at boundary point, *r*, of discretisation in the FILM

δ_{rs} Indentation history for discretisation in the FILM

δ_{tep} Indentation at transition point in the elastoplastic loading stage

δ_y Indentation at yield point

ρ mass per unit area of infinite plate

υ Poisson's ratio